Published in final edited form as:
J Immunol. 2012 February 1; 188(3): 1469–1478. doi:10.4049/jimmunol.1102310.

Role of C3a Receptors, C5a Receptors, and Complement Protein C6 Deficiency in Collagen Antibody-Induced Arthritis in Mice

Nirmal K. Banda[*], **Stephanie Hyatt**[*], **Alexandra H. Antonioli**[*], **Jason T. White**[*], **Magdalena Glogowska**[*], **Kazue Takahashi**[+], **Tod J. Merkel**[±], **Gregory L. Stahl**[§], **Stacey Mueller-Ortiz**[¶], **Rick Wetsel**[¶], **William P. Arend**[*], and **V. Michael Holers**[*]

[*]Division of Rheumatology, Departments of Medicine and Immunology, University of Colorado School of Medicine, Aurora, Colorado, USA

[+]Developmental Immunology, Massachusetts General Hospital for Children, Boston, Massachusetts, USA

[±]Laboratory of Respiratory Pathogens, Division of Bacterial Products, CBER, FDA, USA

[§]Center of Experimental Therapeutics and Reperfusion Injury, Brigham and Women's Hospital, Boston, Massachusetts, USA

[¶]Institute of Molecular Medicine, University of Texas, Houston, USA

Abstract

The complement system, especially the alternative pathway (AP), plays essential roles in the induction of injury in collagen antibody-induced arthritis (CAIA) in mice. The goal of the current study was to directly compare the roles of receptors for C3a and C5a, as well as the membrane attack complex (MAC), as effector mechanisms in the pathogenesis of CAIA. Clinical disease activity (CDA) in *C3aR*$^{-/-}$, *C5aR*$^{-/-}$, and C6 deficient (C6-def) mice was decreased by 52%, 94%, and 65%, respectively, as compared with WT mice. Decreases in histopathologic injury as well as in IgG and C3 deposition paralleled the CDA. A decrease in the percentage of synovial neutrophils was observed in *C3aR*$^{-/-}$, *C5aR*$^{-/-}$, and C6-def mice, and a decrease in macrophages was observed in *C3aR*$^{-/-}$ and *C5aR*$^{-/-}$, but not in C6-def, mice. Synovial mRNA obtained by laser capture microdissection exhibited a decrease in TNF-α in *C5aR*$^{-/-}$ mice and in IL-1β in both *C5aR*$^{-/-}$ and C6-def mice, while *C3aR*$^{-/-}$ mice demonstrated no change in either cytokine. Our findings show that absent C3aR-, C5aR- or MAC-initiated effector mechanisms each decreases susceptibility to CAIA, with clinical effects most pronounced in C5aR deficient mice. Although the absence of C3aR, C5aR, or C6 led to differential deficiencies in effector mechanisms, decreased proximal joint IgG and C3 deposition was common to all three genotypes in comparison to WT mice. These data suggest the existence of positive feedback amplification pathways downstream of all three effectors that promote additional IgG deposition and C3 activation in the joint.

Keywords

autoimmunity; complement; inflammation

Address correspondence to: Dr. V. Michael Holers, Division of Rheumatology, Mail Stop B115, University of Colorado School of Medicine, 1775 Aurora Court, Aurora, Colorado 80045, USA. Phone (303) 724-7605. Fax: 303-724-7581. Michael.Holers@ucdenver.edu.

The online version of this article contains supplemental material.

Introduction

Rheumatoid arthritis (RA) is an inflammatory autoimmune arthritis whose pathogenesis is complex (1, 2). In order to better understand the pro-inflammatory pathways involved in this disease, mouse models of inflammatory arthritis such as collagen-induced arthritis (CIA), anti-GPI Ab-induced arthritis (anti-GPI Ab) and collagen Ab-induced arthritis (CAIA) have been devised and studied extensively. Our laboratory, along with others, has shown a significant and necessary role for the alternative pathway (AP) of complement in the pathogenesis of inflammatory arthritis in mice (3–9).

Complement is a potent effector pathway of innate immunity that accomplishes its biologic roles in inflammation by using several key pro-inflammatory and immunomodulatory mechanisms. C3 and C5 are central pillars of this system. For example, all three activation pathways of the complement system converge to form a C3 convertase, or activating enzyme, which cleaves C3 into the C3a and C3b fragments. The generation of C3b leads to the formation of another enzyme, the C5 convertase, which then cleaves C5 into the C5a and C5b fragments. C3a and C5a fragments are the most potent pro-inflammatory anaphylatoxins generated during complement pathway activation. These anaphylatoxins recruit and/or activate monocytes/macrophages and neutrophils, which themselves are involved in a myriad of pathologic states including those of autoimmune diseases, inflammatory reactions, allergic reactions, asthma, and cancer (10–14). In addition to anaphylatoxins, through the formation of the membrane attack complex (MAC) the complement system eliminates pathogens through lysis and causes local tissue injury by the initiation of pro-inflammatory signaling in cells.

C3a and C5a induce their biological actions through two specific receptors designated the C3aR and C5aR (CD88), respectively (15, 16). C5L2 (GPR77) is another non-signaling receptor for C5a (17–19), which likely acts as a decoy receptor and a negative modulator of C5a-induced responses (20). Both major receptors for C3a and C5a belong to a family of transmembrane G protein coupled receptors, but C5L2 is not coupled to the G proteins (17, 21). Many different cell types express receptors for C3a and C5a. These include cells of myeloid origin (22), non-myeloid origin (23), dendritic cells (24), monocyte/macrophages (25), and neutrophils (26). Resting mast cells express C5aR below threshold levels, but stimulation with phorbol myristate acetate (PMA) or ionomycin results in increases in C5aR expression as well as in slight increases in C3aR receptors (27).

Following C5b generation, C6 interacts with C5b on the cell surface to begin formation of the MAC (C5b, C6, C7, C8α, C8β, C8γ, and C9) that can insert into any cell membrane (28). Deficiency of any of the aforementioned proteins of the MAC would block the formation of the lytic complex in the membrane of cells. If present at high enough levels, the MAC causes lysis of cells; perhaps more importantly, when present in sublytic concentrations, the MAC also transduces pro-inflammatory cell activation signals (29). The MAC also plays a role in the cell cycle and apoptosis (30, 31) and has been shown to be present in RA tissue, suggesting a role in the pathogenesis of arthritis (32).

Serum-induced arthritis in K/BxN mice is mediated by anti-GPI-immunoglobulins (Igs) (33) and the development of disease requires both C5aR and FcγIII receptors (7). This study also showed that disease was dependent on the AP of complement. On the other hand, C6-deficient (C6-def) mice on a C3H/He background were fully susceptible to anti-GPI Ab-induced arthritis (7), suggesting a lack of role for the MAC. In contrast, there was a 60% decrease in monosodium urate monohydrate (MSU) crystal-induced arthritis in NZW rabbits deficient in C6 (34). This study reported infiltration of mononuclear leukocytes in the synovial tissue in all animals, but substantial infiltration of neutrophils was also seen in C6-

def rabbits in response to MSU crystals. In addition, in a mouse model of choroidal neovascularization (CNV), i.e. laser-induced CNV which involves inflammation, anti-C6 mouse polyclonal Ab inhibited the formation of the MAC and resulted in amelioration of CNV (35). Anti-C6 Fab also reduced experimental autoimmune myasthenia gravis disease passively induced in rats (36), showing the dependency of this disease on MAC formation.

Despite this body of work on the role of individual effector pathways, no prior study has directly compared the relative roles of C3aR, C5aR, and the MAC in the development of tissue injury in any single disease model. The purpose of the current study was to explore the relative roles of these three major effector pathways in CAIA in C57BL/6 mice. Our hypothesis was that the interactions between C3a-C3aR and C5a-C5aR, and a deficiency of MAC formation, would result in differential effector function and thus lead to different disease phenotypes in *C3aR*$^{-/-}$, *C5aR*$^{-/-}$, and C6-def mice. Although we found that each effector demonstrated unique characteristics with regard to changes in downstream pro-inflammatory effects in their absence, there were similar ameliorative effects on the disease course itself. One unexpected feature shared by all effector deficient mice was decreases in the levels of local IgG and C3 deposition in the joint.

Materials and Methods

Mice

Ten to twelve week-old homozygous *C3*$^{-/-}$, *C3aR*$^{-/-}$, *C5aR*$^{-/-}$, and C6-def C57BL/6 male and female mice were used for this study of CAIA. *C3aR*$^{-/-}$and *C5aR*$^{-/-}$ mice were obtained from Dr. Rick Wetsel, University of Texas, Houston, and C6-def mice were obtained from Dr. Tod Merkel, CBER, FDA. Because C57BL/6 mice naturally lack complement protein C6 and are not gene-targeted mice, in the current studies these mice have been designated as C6 deficient (C6-def). These C6-def C57BL/6 mice have been derived from a C6-def C3H/He mouse strain, as narrated in detail below. Sera from *C1q*$^{-/-}$, *C3*$^{-/-}$, *C4*$^{-/-}$, *Bf*$^{-/-}$, and *Df*$^{-/-}$ mice backcrossed to at least F10, as well as C5-deficient NOD (non-obese diabetic) mice, were used as negative controls in ELISA assays as described. Age- and sex-matched C57BL/6 mice (Jackson Labs, Bar Harbor, ME) were used as wild type (WT) controls. Genotypes of deficient strains were confirmed by deletion-specific DNA PCR analysis prior to use of the animals. The studies were performed in four different cohorts with the following total mice studied: WT n = 25, *C3*$^{-/-}$ n = 4, *C3aR*$^{-/-}$ n = 13, *C5aR*$^{-/-}$ n = 11, C6-def n = 8. All animals were kept in a barrier animal facility with a climate-controlled environment providing 12 h light/dark cycles. Filter top cages were used with three mice in each cage. During the course of this study, all experimental mice were fed breeder's chow provided by the Center for Laboratory Animal Care, University of Colorado School of Medicine.

Derivation of C57BL/6 C6-def mice

C6-def C3H/He mice were derived from a Peru-Peacock strain of mice that lacked functional C6 (37). The molecular basis of the deficiency was determined to be due to the presence of several base-substitutions in the C6-deficient allele relative to the wild-type allele (38). These base-substitutions result in the presence of restriction enzyme site *Bst*NI in the wild-type allele that is absent in the C6-def allele and the presence of restriction enzyme site *Alw*NI in the C6-def allele that is absent in the wild-type allele. This allowed for unambiguous identification of heterozygous mice, mice homozygous for the C6-def allele, and mice homozygous for the wild-type allele. Genomic DNA was isolated from whole blood from individual mice using the MoBio UltraClean DNA BloodSpin Kit kit (MO BIO Laboratories Inc., Carlsbad, California) according to the manufacturer's instructions. DNA amplification was performed using primers C6DE-F1

(5'GACCCTTGCCAGTGTGCTCCATGTCCCA-3' and C6DE-R1 (5'-GGACCTGCGCTCACAGTTCTCA-3') using Roche PCR Master Mix (Roche Applied Science, Indianapolis, Indiana) according to the manufacturer's instructions. The resulting PCR product was gel purified and independently digested with restriction enzymes *Bst*NI and *Alw*NI. The restriction patterns for each digestion were analyzed to determine whether the wild-type allele or the C6-allele, or both alleles, were present. In order to transfer the C6-def allele to the C57BL/6 background, C6-def C3H/He mice were backcrossed 8 times to C57BL/6 mice. Following each backcross, offspring homozygous for the C6-deficient allele were identified using the PCR/restriction enzyme screen described above and crossed with wild-type C57BL/6 mice. Following the eighth backcross, offspring homozygous for the C6-deficient allele were selected and used to set up homozygous breeding pairs. The offspring of these breeding pairs were confirmed to be homozygous for the C6-deficient allele using the PCR/restriction enzyme screen described above and were determined to be deficient for complement-mediated lysis in a red blood cell assay and to lack C6 protein by Western blot (data not shown). A coagulation defect, characterized as decreased platelet aggregation, was described in the original C6-def C3H/He mice, corrected by adding purified rat C6 protein *in vitro* (38). It is not known if a similar coagulation defect is present in the C6-def C57BL/6 mice used in this study.

Induction of collagen antibody-induced arthritis

CAIA was induced in $C3aR^{-/-}$, $C5aR^{-/-}$, and C6-def, and WT mice by using a cocktail of five mAb to bovine CII (Arthrogen-CIA, Chondrex) suspended in sterile Dulbecco's PBS. All five mAb (3 IgG2a and 2 IgG2b) in this cocktail recognize conserved epitopes within the CB11 fragment, whose recognition sequences are shared by CII in many species. All mice received i.p. injections of 8 mg/mouse of Arthrogen on day 0 and 50 μg/mouse of LPS from E. coli strain 0111B4 on day 3 to synchronize the development of arthritis. Mice started to develop arthritis at day 4 and were sacrificed at day 10. The studies were performed in four separate experiments. The first experiment consisted of $C3aR^{-/-}$ (n = 5), $C5aR^{-/-}$ (n = 5), and WT (n = 6) mice; the second consisted of $C3aR^{-/-}$ (n = 3), $C5aR^{-/-}$ (n = 2), C6-def (n = 3), and WT (n = 4) mice; the third consisted of $C3aR^{-/-}$ (n = 5), $C5aR^{-/-}$ (n = 4), and WT (n = 4) mice; and the fourth consisted of C6-def (n = 5) and WT (n =11) mice. For presentation of results, all genotype identical mice were grouped together from each of the four experiments and included in the final analyses.

Examination for clinical disease activity

The prevalence of disease and severity of clinical disease activity (CDA) in all $C3aR^{-/-}$, $C5aR^{-/-}$, C6-def, and WT mice were determined every day by a trained laboratory person blinded to the experimental treatment group according to our previously published studies (5). The CDA score is based on a 3 point scale per paw: 0 = normal joint; 1 = slight inflammation and redness; 2 = severe erythema and swelling affecting the entire paw with inhibition of use; and 3 = deformed paw or joint with ankylosis, joint rigidity and loss of function. The total CDA score was based on all 4 paws with a maximum total of 12 for each mouse.

Histopathology and immunohistochemistry for C3 and IgG

Knee joints from both fore limbs, and the right hind limb with knee joint, ankle and paw, from $C3aR^{-/-}$, $C5aR^{-/-}$, C6-def, and WT mice at day 10 following Arthrogen injection were fixed in 10% Neutral buffered formalin (NBF). Toluidine-blue stain was used to assess histopathology scores for inflammation, pannus formation, cartilage and bone damage, according to the published criteria (39, supplemental data). Histology sections were cut (7 μm) and processed for C3 and IgG immunohistochemistry staining. Non-specific binding was blocked using a protein block serum free solution (Dako). C3 was localized with a

primary polyclonal goat anti-mouse C3 antiserum (dilution 1:10,000) (ICN Pharmaceuticals) and detected by goat HRP polymer kit (BioCare Medical) (5). IgG was localized with a primary polyclonal goat anti-mouse Ab (dilution 1:200) (Vector Laboratories, Burlington, CA) and detected by a goat HRP polymer kit, as mentioned above. Development of staining identifying the presence of tissue-fixed C3 and IgG was carried out using DAB plus solution substrate (Dako), which reacts with HRP and produces a brown color for positive staining. All slides for histopathology, C3 and IgG deposition were observed under light microscopy at a magnification of 20X in a blinded fashion and scored according to published criteria (39). IgG deposition on the surface of cartilage in the knee joints of WT, *C3aR*$^{-/-}$, *C5aR*$^{-/-}$, and C6-def mice with disease was determined by using the following scale: 0 = normal WT with no disease, i.e. background endogenous mouse IgG staining, 1 = minimum staining, 2 = moderate staining, and 3 = intense staining. The knee joints from *RAG2*$^{-/-}$ mice on C57BL/6 background with no disease were also used as negative controls.

Quantitative assessment of monocytes/macrophages and neutrophils in the knee joints

Histology sections from the knee joints of all *C3aR*$^{-/-}$, *C5aR*$^{-/-}$, C6-def, and WT mice with CAIA sacrificed at day 10 were also examined for the infiltration of monocytes/macrophages and neutrophils in the knee joints. To determine the percentages of monocytes/macrophages and neutrophils, sections were pre-treated with proteinase K (0.05 mol/L) (Dako) for 5 min for Ag retrieval, followed by blocking with a serum free protein block solution (no dilution) (Dako). Immunohistochemistry analysis for monocytes/macrophages was performed by staining sections with rat anti-mouse F4/80 (dilution 1:1000) (Serotec) and rabbit anti-rat (dilution 1:400) (Dako), as primary and secondary Ab, respectively. Rabbit Alkaline Phospatase Polymer (ALP) (no dilution) (BioCare Medical) was used as a tertiary Ab. Detection of monocytes/macrophages was performed using Vulcan Fast Red Chromogen (no dilution) (BioCare Medical). To determine the percentage of neutrophils, knee joint sections were stained with a primary rat anti-mouse neutrophil Ab (dilution 1:2000) (Serotec) and a secondary rabbit anti-rat Ab (dilution 1.400) (Dako), followed by Rabbit Envision Polymer (no dilution) (HRP conjugated) (Dako). Neutrophils were detected by using 3,3'-diaminobenzidine (DAB+) (no dilution) (Dako). The percentages of the monocytes/macrophages and neutrophils were calculated by marking the boundaries of synovium using Scan Scope XT (Aperio). The formula used to calculate such percentages was the total number of positively stained synovial area/total marked synovial area x100. Although the areas of synovium were heterogeneous due to inflammation, all stained areas were included in assessing percentages of monocytes/macrophages and neutrophils.

Measurement of C3 deposition and C5a generation in vitro using sera from mice

Complement activity in sera from *C3*$^{-/-}$, *C3aR*$^{-/-}$, *C5aR*$^{-/-}$, C6-def, NOD, and WT mice was assayed *in vitro* by measuring C3 deposition and C5a generation. Blood for these studies was collected by retro-orbital bleeding and allowed to clot for 30 min at 4°C. After centrifugation at 3000 rpm for 15 min at 4°C, sera were separated from the clot on ice and were kept at −70°C immediately after collection until further analysis. To avoid complement activation, sera were used only one time without being subjected to repeated cycles of freezing and thawing. Sera were discarded that showed any discoloration due to hemolysis. Frozen serum samples were thawed at 4°C and the diluted sera were kept on ice prior to use. For analysis of all three pathways of complement activation, sera were serially diluted 2-fold from 1:10 in Ca^{++}-sufficient buffer for C3b deposition and serially diluted 2-fold from 1:50 for C5a generation. To study specific activation of the AP only, the same sera were serially diluted 2-fold in Ca^{++}-deficient buffer containing Mg^{++}/EGTA. These sera were then added to 96-well Costar ELISA plates pre-coated with anti-CII mAb (Arthrogen, 2.5 ug/well) and incubated at 37° C for 1 h. C3 deposition adherent to the plate and C5a generation in the supernatant were measured by ELISA, as previously described (4, 39).

Levels of complement components in the sera from complement-deficient and WT mice

Serum levels of C1q, C4, C3, factor B and factor D proteins from *C3aR*$^{-/-}$, *C5aR*$^{-/-}$, C6-def, and WT mice were measured using standard ELISA protocols, according to our published methods (4, 39).

Cytokine mRNA levels from the synovium of knee joints using laser capture micro-dissection (LCM)

The left knee joint was surgically removed from mice with and without CAIA at day 10, the skin was removed, and the tissue was placed in liquid nitrogen. After removing extra muscle using a surgical blade, the knee joint was embedded for 5 min in Tissue-Tek® O.C.T.™ Compound (Sakura Finetek, The Netherlands). The histology sections were cut at 8 micron thickness (Leica Microsystems, Wetzlar, Germany) and mounted onto Histobond® slides (Statlab Medical Products, McKinney, TX). All slides were dehydrated for 30 sec sequentially in 70%, 95%, and 100% ethanol, and for 5 min in xylene (Arcturus® Histogene®, Carlsbad, CA). The slides were rehydrated in nuclease-free water (Arcturus® Histogene®) containing 50 μL of RNase inhibitor (Sigma-Aldrich, St. Louis, MO) for 30 sec to remove the O.C.T. compound. The slides were air-dried for 5 min. The knee joint was located at 2X magnification and the synovium was viewed at 10X. The capture Macro LCM Cap (Arcturus Histogene®) was placed on the area around the identified synovium. The histo-pencil from the drawing tools was used to mark the boundaries of the synovium to be placed on the cap, and an infrared laser was fired. The infrared laser melted the polymer onto the cap creating an adhesion of the cells to the polymer. The cap was moved to the quality control station to view the synovium. The cap with the synovium was placed in a tube with 50 μL of RNA extraction buffer (Arcturus® Histogene®) and incubated for 30 min at 42°C. RNA was isolated using the PicoPure RNA isolation kit (Arcturus® Histogene®), and then amplified (1.5–2.0 round amplification) using the RiboAmp Plus kit (Arcturus® Histogene®) by synthesizing cDNA strands from the isolated RNA with enhancers and transcribing it into amplified RNA (aRNA). The aRNA was purified using a column method supplied in the kit. RNA concentration was measured using a nanodrop. This aRNA was then used for quantitiative RT-PCR using specific primers for the mRNA levels of TNF-α, IFN-γ, IL-1β, and IL-10, as previously published (5, 39)

Statistical analyses

p-values were calculated using Student's t test with the GraphPad Prism^{R} 4 statistical program. The data in graphs, histograms and tables are shown as the mean ± SEM, with $p < 0.05$ considered significant using an unpaired two-tailed t-test. One-way analysis of variance (ANOVA) using Tukey's multiple comparison test was also performed to further confirm the significant differences between WT, *C3aR*$^{-/-}$, *C5aR*$^{-/-}$, and C6-def mice for CDA, histology, C3 deposition/C5a generation, and QRT-PCR data. Pearson correlation was used to determine the correlation between CDA, neutrophils, macrophages, histology, and absolute serum complements levels. Preliminary analyses using a null hypothesis for w-statistics indicated that the data were usually normally distributed. Where data were not normally distributed, the Mann-Whitney test was used.

Results

Clinical disease activity and prevalence of disease

CDA in all cohorts of mice was evaluated every day after the LPS injection on day 3. Mice injected with Arthrogen developed disease after day 3, and at day 10 the CDA in WT, *C3aR*$^{-/-}$, and *C5aR*$^{-/-}$ mice were 10.8 ± 0.54, 5.2 ± 1.1, and 0.64 ± 0.20, respectively (Fig. 1A). These scores were significantly reduced by 52% and 94% in *C3aR*$^{-/-}$ and *C5aR*$^{-/-}$

mice, respectively, as compared to WT mice. The prevalence of disease at day 10 in WT, *C3aR*$^{-/-}$, and *C5aR*$^{-/-}$ mice was 100%, 85%, and 55%, respectively (Fig. 1B). At day 10 the CDA in WT and C6-def mice was 9.3 ± 0.66 and 3.3 ± 0.41, respectively (Fig. 1C). The CDA in C6-def mice was significantly reduced by 65% as compared to WT mice. The prevalence of disease at day 10 both in WT and C6-def was 100% (Fig. 1D). *C5aR*$^{-/-}$ mice were more resistant to the development of CAIA as measured by CDA than *C3aR*$^{-/-}$ mice and C6-def mice ($p < 0.01$). No statistically significant ($p = 0.18$) difference was observed when comparing CDA between *C3aR*$^{-/-}$ and C6-def mice.

Differential patterns of disease development in C3aR$^{-/-}$ mice

We examined CDA in each mouse from day 3 to day 10 in all four cohorts of mice. There were only scattered individual variations of CDA in *C5aR*$^{-/-}$ and *C6*$^{-/-}$ mice (Figs. S1, panels C and D). However, there was substantial variation in the individual CDA in WT and *C3aR*$^{-/-}$ mice (Fig. S1, panels A and B). Four *C3aR*$^{-/-}$ mice developed severe disease similar to the WT mice, while five mice developed moderately high levels of disease and four mice developed minimal levels of disease. This variation in the CDA in *C3aR*$^{-/-}$ mice was found consistently in all three cohorts tested. The genotype of the mice was confirmed twice as *C3aR*$^{-/-}$ prior to the induction of CAIA by PCR using genomic DNA.

Histopathology, C3 and IgG deposition scores in forelimbs and hind limbs

All mice were sacrificed at day 10, after which both forelimbs and the right hind limb (knee, ankle and paw) were processed for histopathology studies (Figs. 2A and 2B), for measurement of local C3 deposition (Figs. 2C and 2D), and for IgG deposition (Fig 3). Five joints from WT, *C3aR*$^{-/-}$, *C5aR*$^{-/-}$, and C6-def mice used in this study were examined for inflammation, pannus formation, cartilage damage and bone damage (Figs. 2A and 2B). Individual scores for these parameters were all significantly ($p < 0.05$) decreased in *C3aR*$^{-/-}$ and *C5aR*$^{-/-}$ compared with WT mice (Fig. 2A). In addition, all joint mean (AJM) scores for histopathology were significantly ($p < 0.001$) reduced by 44% and 57% in *C3aR*$^{-/-}$ and *C5aR*$^{-/-}$ mice, respectively, compared with the WT mice (WT 14.07 ± 0.544, *C3aR*$^{-/-}$ 7.86 ± 0.66, and *C5aR*$^{-/-}$ 6.02 ± 0.17). Individual scores for inflammation, pannus formation, cartilage and bone damage were also significantly ($p < 0.05$) decreased in C6-def compared with WT mice (Fig. 2B). Similarly, there was a significant decrease by 39% in the AJM histopathology scores in C6-def mice compared with the WT mice (WT 12.07 ± 0.947 and C6-def 7.35 ± 0.73). *C5aR*$^{-/-}$ mice have significantly less inflammation vs. *C3aR*$^{-/-}$ mice ($p < 0.0078$) and vs. C6-def mice ($p < 0.017$), less pannus formation vs. *C3aR*$^{-/-}$ mice ($p < 0.012$) and vs. C6-def mice ($p < 0.023$), and less cartilage damage vs. *C3aR*$^{-/-}$ mice ($p < 0.041$) (Figs. 2A and 2B). All joint mean scores were also significantly reduced in *C5aR*$^{-/-}$ mice vs. *C3aR*$^{-/-}$ ($p < 0.020$) and vs. C6-def mice ($p < 0.049$). No significant reduction in cartilage and bone damage was observed between *C5aR*$^{-/-}$ and C6-def mice. Representative histopathologic examples of the knee joints from WT, *C3aR*$^{-/-}$, *C5aR*$^{-/-}$, and *C6*$^{-/-}$ mice are shown in Fig. 4 (A, B, C and D).

Deposition of C3 and IgG was specifically examined in the knee joints of all WT, *C3aR*$^{-/-}$, *C5aR*$^{-/-}$, and C6-def mice. No C3 deposition was present in the knee joints of control WT and *C3*$^{-/-}$ mice without CAIA (Fig. S2). Similarly, no C3 deposition was present in the knee joints of control *C5aR*$^{-/-}$, *C3aR*$^{-/-}$, and C6-def mice without CAIA (data not shown). C3 deposition in the synovium and in the cartilage was significantly reduced in the knee joint of *C3aR*$^{-/-}$ and *C5aR*$^{-/-}$ mice compared with WT (Fig. 2C), and was also reduced significantly in the synovium and cartilage of C6-def mice compared with WT mice (Fig. 2D), all with CAIA. AJM scores (synovium and cartilage) for C3 deposition were reduced by 41%, 57% and 30% in *C3aR*$^{-/-}$, *C5aR*$^{-/-}$, and C6-def mice, respectively, compared with WT mice with CAIA. With regard to individual compartments, C3 deposition in the

synovium of *C3aR*$^{-/-}$, *C5aR*$^{-/-}$, and C6-def mice compared with the WT mice was decreased by 37%, 55%, and 23%, respectively (Figs. 2C and 2D). C3 deposition on the cartilage surface of *C3aR*$^{-/-}$, *C5aR*$^{-/-}$, and C6-def mice compared with the WT mice was decreased to 45%, 60%, and 42%, respectively (Figs. 2C and 2D). The correlations (r) between AJM C3 deposition in the knee joints and CDA at 95% CI in WT, *C3aR*$^{-/-}$, *C5aR*$^{-/-}$, and C6-def were 0.57 ($p < 0.0017$), 0.90 ($p < 0.001$), 0.65 ($p < 0.027$), and 0.53 ($p < 0.18$), respectively. There was more decrease in C3 deposition (all joint mean score) in the synovium as well as on the cartilage surface in the knee joint of *C5aR*$^{-/-}$ mice than in *C3aR*$^{-/-}$ ($p < 0.016$) and C6-def ($p < 0.0027$) mice (Fig 2). Representative C3 deposition pictures of the knee joints from WT, *C3aR*$^{-/-}$, *C5aR*$^{-/-}$, and C6-def mice are shown in Fig. 4 (E, F, G and H).

IgG deposition was specifically examined in the knee joints of all WT, *C3aR*$^{-/-}$, *C5aR*$^{-/-}$, and C6-def mice. No IgG deposition was observed in the synovia of these mice. Representative IgG deposition pictures on the surface of cartilage from the knee joints of WT, *C3aR*$^{-/-}$, *C5aR*$^{-/-}$, and C6-def mice are shown in Fig. 3A (1, 2, 3 & 4). Representative IgG deposition pictures on the surface of cartilage from the knee joints of C57BL/6 WT mice without CAIA and *RAG2*$^{-/-}$ C57BL/6 mice without CAIA are shown in Fig. 3A (panels 5 and 6). IgG deposition on the surface of the cartilage was significantly ($p < 0.001$) reduced in the knee joints from *C3aR*$^{-/-}$ and *C5aR*$^{-/-}$ mice, but not in C6-def mice, in comparison with the WT mice with CAIA (Fig. 3B). Endogenous IgG present on the cartilage of knee joints from WT and *RAG2*$^{-/-}$ mice without CAIA was considered as the baseline background.

C3 deposition and C5a generation induced by anti-collagen antibodies in vitro

Sera from WT, *C3aR*$^{-/-}$, *C5aR*$^{-/-}$, and C6-def mice were used for in vitro studies on complement activation. To study activation by all three complement pathways, sera were serially diluted 2-fold from 1:10 for C3b generation, and from 1:50 for C5a generation, in buffer containing Ca^{++}. To analyze activation by the AP only, sera were serially diluted 2-fold in buffer in the absence of Ca^{++} with Mg^{++}/EGTA. Serial two-fold dilutions of sera were incubated on plates with adherent anti-CII mAb and C3 deposition on the ELISA plate and C5a generation in the supernatant were measured (Fig. 5). Negative controls included NOD sera naturally lacking C5 and sera from *C3*$^{-/-}$ mice. With Ca^{++}-sufficient buffer, equivalent levels of C3 deposition were observed using all sera except for sera from *C3*$^{-/-}$ mice where no C3 deposition was observed, as expected (Fig. 5A). Levels of C5a generation in the presence of Ca^{++} were slightly lower using sera from *C3aR*$^{-/-}$, *C5aR*$^{-/-}$, and C6-def mice in comparison to WT, and were absent using sera from NOD mice (Fig. 5B). In the absence of Ca^{++}, where only the AP was active, levels of C3b deposition and of C5a generation were slightly lower using sera from C6-def mice in comparison to WT (Figs. 5C and D).

Assessment of macrophage and neutrophil infiltration in the synovium of knee joints from mice with CAIA

The infiltration of macrophages and neutrophils in the knee joint synovium from WT, *C3aR*$^{-/-}$, *C5aR*$^{-/-}$, and C6-def mice was determined using immunohistochemical methods with specific cell surface markers, as outlined in the Methods. The percentages of macrophages and neutrophils were decreased significantly in the synovium of *C3aR*$^{-/-}$ and *C5aR*$^{-/-}$ mice with CAIA in comparison with the WT mice (Fig. 6). The decrease in synovial macrophages in *C3aR*$^{-/-}$ and *C5aR*$^{-/-}$ as compared with the WT mice with disease was 20% ($p < 0.005$) and 35% ($p < 0.001$), respectively. A more dramatic decrease in the percentages of synovial neutrophils was observed in *C3aR*$^{-/-}$, *C5aR*$^{-/-}$, and C6-def mice with disease as compared to WT mice with decreases of 56% ($p < 0.014$), 72% ($p < 0.002$),

and 57% ($p < 0.044$), respectively. No statistically significant decrease was seen in the percentages of synovial macrophages in $C6^{-/-}$ mice with disease as compared with WT mice with disease (Fig. 6). Representative examples of neutrophil and macrophage infiltration are shown in Fig. 4 (panels I–L and M–P, respectively).

Cytokine mRNA from synovium obtained by LCM from the knee joints of mice with disease

mRNA levels were evaluated by quantitative RT-PCR using cDNA made from the amplified mRNA (aRNA) obtained using LCM from the synovium of the left hind limb of WT, $C3aR^{-/-}$, $C5aR^{-/-}$, and C6-def mice (Fig. 7). No significant differences were seen in the levels of TNF-α mRNA in the synovium of $C3aR^{-/-}$, and C6-def mice with disease (Fig. 6A). In contrast, a significant decrease ($p < 0.011$) was observed in the levels of TNF-α mRNA in the synovium of $C5aR^{-/-}$ mice in comparison to WT mice (Fig. 7A). Significant decreases in levels of IL-1β mRNA were also seen in the synovium of $C5aR^{-/-}$ ($p < 0.046$) and C6-def ($p < 0.005$) mice, but not *C3aR-/* mice, in comparison to WT mice (Fig. 7B).

Absolute levels of complement components in mice sera

The absolute levels of various complement components such as C1q, C4, C3, factor B and factor D were measured in sera from WT, $C3aR^{-/-}$, $C5aR^{-/-}$, and C6-def mice (Table 1). No major decreases in the levels of complement proteins were observed that might provide alternative explanations for differences in CDA and histologic changes in these strains. However, decreases of 35%, 32%, and 26% in the absolute levels of C4 were seen in the sera from $C5aR^{-/-}$ mice in comparison with sera from WT, $C3aR^{-/-}$, and C6-def mice, respectively. The decrease in the levels of C4 in sera from $C5aR^{-/-}$ mice compared with WT mice was significant ($p < 0.014$).

Discussion

The primary goal in this study was to compare the roles of the C3aR, C5aR, and MAC (C5b-9) in the pathogenesis of inflammatory arthritis using an identical mouse model, (CAIA), in a single strain of C57BL/6 mice. We found that each of the three effector mechanisms initiated by the C3aR, C5aR, or the MAC was essential to the full development of arthritis; deficiency states in each of the three resulted in significant amelioration in both the primary clinical and histopathologic disease endpoints. The lack of C5aR showed the greatest decreases in CDA and parameters of histological change in these studies. Previous studies demonstrated no effect of a deficiency in the C3aR on CAIA on the Balb/c background (40), and a lack of effect of C6-def in anti-GPI-induced arthritis in the C3H/He background (7). Nevertheless, our current studies in C57BL/6 mice have demonstrated a substantial role for C3aR as well as a comparably important role of the MAC in CAIA, pointing out the importance of evaluating more than one strain of mice and model before concluding a lack of effect of a particular complement effector pathway.

We observed some key differences in the specific downstream effects of each mechanism of inflammation and tissue destruction. A significant decrease in the percentage of synovial neutrophils was observed in $C3aR^{-/-}$, $C5aR^{-/-}$, and C6-def mice, and a decrease in macrophages was observed in both $C3aR^{-/-}$ and $C5aR^{-/-}$, but not in C6-def, mice. In addition, a significant decrease in TNF-α mRNA levels was observed in the synovium of $C5aR^{-/-}$ mice, and a decrease in IL-1β mRNA in both $C5aR^{-/-}$ and C6-def mice, while $C3aR^{-/-}$ mice demonstrated no changes in either cytokine. These results may reflect the effects of different expression of the two receptors or of alternate receptors for C3a and C5a, differences in signal transduction pathways that follow engagement of C3aR, C5aR, and the G-protein linked pathways that are subsequently activated, or differences in the numbers or

types of infiltrating cells. However, the specific mechanisms involved in absent expression of mRNA for TNF-α and IL-1β in particular strains of gene-deficient mice remain unknown.

Neutrophil activation through C5aR in CAIA, possibly acting synergistically through enhancement in activating Fc receptors, likely plays an important role in the differential effects following chemotactic peptide engagement. This conclusion is supported by data from other experimental models of arthritis initiated by immune complexes where the absence of receptors for C5a on the surface of neutrophils in *C5aR*$^{-/-}$ mice likely resulted in the observed decrease in infiltration of neutrophils (39). In addition, mouse neutrophils and macrophages are known to express C5aR (41) and upon contact with human recombinant C5a mononuclear phagocytes release TNF-α and IL-1β (42). Thus, with a decrease in synovial neutrophils and the lack of a C5aR signal, the absence of detectable mRNAs for these cytokines in our studies is not unexpected.

Alternatively, in the absence of C5aR there may be counter-regulatory mechanisms available such as the existence of C5L2 receptors that would interact with the available C5a. It has been shown that *C5aR*$^{-/-}$ mice that also express C5L2 receptors alone do not respond with a pro-inflammatory phenotype to C5a (21). This receptor may thus serve to modulate C5a biological functions *in vivo*. In addition to the potential effects of C5L2, blockade of C5aR on alveolar macrophages in lung Arthus reactions led to an increased ratio of FcγRIIB (inhibitory) to FcγRIII (activating) receptors (43). Therefore, local inhibition of lung C5aR can abrogate inflammation by increasing the relative expression ratio of the inhibitory receptor FcγRIIB.

Despite the major role for C5a and C5aR, deficiencies in either C3aR or MAC function in our studies also led to substantial decreases in the CDA and joint histologic injury scores. Consistent with this outcome, receptors for C3a are also present on murine monocytes/macrophages and neutrophils. It was shown that C3a stimulation of non-adherent PBMCs suppressed LPS-induced mRNA levels of TNF-α and IL-1β whereas C3a stimulation of adherent PBMCs led to enhanced LPS-induced TNF-α and IL-1β mRNA levels (44). Thus, C3a causes cytokine release from many cell types in vitro including IL-1β and TNF-α (44). However, the absence of changes in the levels of these cytokines in *C3aR*$^{-/-}$ mice suggests that the C5a that is generated is able to provide a sufficient signal in the absence of C3aR. Alternatively, it has also been shown that C3a binds to the receptor for advanced glycation end products (RAGE) (45). In CIA, the expression of RAGE is increased and synovial tissue inflammation, cartilage and bone destruction are decreased by treatment with soluble RAGE (46). Therefore, the more modest decrease in disease in *C3aR*$^{-/-}$ mice might be due to the availability of alternate receptors for C3a, such as RAGE, on the surface of effector cells. In this instance, the high levels of TNF-α and IL-1β in the synovium from the knee joints of *C3aR*$^{-/-}$ with CAIA may be due in part to the binding of C3a to RAGE on macrophages.

Another unexpected result, based on prior studies of anti-GPI-induced arthritis, was our finding of protection from CAIA in the presence of C6 deficiency and the resulting absence of the MAC. One explanation may be that, despite the influx of macrophages and the presence of TNF-α in the knee joints of C6-def mice with CAIA that was similar to WT mice, the influx of neutrophils was reduced. Thus, partial protection of C6-def mice from CAIA may be dependent on decreased neutrophils and not on macrophages. Our studies are also consistent with the results of previous studies on experimental models of arthritis in rats or myasthenis gravis in rabbits where it was shown that C6 deficiency effectively reduced disease severity (34, 36). An important direct or bystander role for MAC in inflammatory arthritis may be the induction of cytokines. This is supported by the minimal levels of IL-1β mRNA in the joints in C6-def mice with CAIA.

It should be emphasized that C6 deficiency was originally described in the Peru-Coppock strain, which were then backcrossed for 10 generations into the C3H/He strain (37). Thus, the C6 deficiency is due to a spontaneously occurring mutation, not to a specific induced gene deletion. The mice used in this study were obtained by backcrossing C6-def C3H/He mice into the C57BL/6 strain for 8 generations. A defect in coagulation, characterized as impaired platelet aggregation, was described in C6-def C3H/He mice and was reversed in vitro by restoration with purified rat C6 protein (38). The coagulation and complement systems are known to exhibit interactions and the possibility exists that platelet aggregation in rodents is dependent on the terminal components of the complement system. To our knowledge, a similar defect in platelet aggregation has not been examined for in C6-def C57BL/6 mice and theoretically, if present, may have influenced our observations.

One striking finding common to mice with deficiencies in mice lacking C3aR or C5aR was a decrease in local IgG and C3 deposition in the joint in comparison to WT mice. Since each effector pathway is “downstream” of C3 activation, it would seem that joint IgG and C3 deposition levels would be comparable between WT and mice with complement deficiencies. Nevertheless, this was not the case, suggesting that WT mice hypothetically may possess mechanisms that enhance IgG deposition with subsequent binding of C3. Thus, WT mice may exhibit increased migration of IgG into the joints and/or greater deposition of the anti-CII mAb. In other studies, C5-deficient mice failed to develop CAIA, although deposition of anti-CII mAb and C3 on the cartilage surface was unchanged (47). This finding indicates that the dependency of CAIA on C5 may be due to increased chemotaxis of neutrophils and macrophages into the joint.

The increased deposition of IgG in the joints of WT mice in the present studies, in comparison to mice with the three complement deficiencies, suggests the possibility of degradation of collagen by enzymes from phagocytic cells. This breakdown could expose new epitopes to which further anti-CII mAb could bind (47–49), leading to additional C3 fixation with further amplification of local complement activation through the AP. The explanation seems less likely that the increased IgG and C3 deposition in WT mice was secondary merely to the enhanced inflammation since these conditions would lead to further enzymatic degradation of deposited IgG and C3. A possibility also exists that IgG is processed or cleared more rapidly in *C3aR*$^{-/-}$, *C5aR*$^{-/-}$, and *C6*-def mice in comparison to WT mice. A slower rate of IgG clearance in WT mice could hypothetically lead to more deposition in joints over time. Studies are in progress to study rates of IgG clearance in mice deficient in C3aR, C5aR, or C6 protein.

We observed that serum levels of C4 were decreased in *C5aR*$^{-/-}$ mice. Similar decreases in serum C4 levels were previously found in *C1q*$^{-/-}$, *C3*$^{-/-}$, *MBL*$^{-/-}$, and *Bf*$^{-/-}$ mice, and the mechanisms remain unexplained (3). Nevertheless, the absence of changes in C3 deposition, and a slight decrease in generation of C5a, in vitro using sera from *C5aR*$^{-/-}$ mice suggests that the decrease in C4 levels should not have affected the in vivo results.

Lastly, mice genetically deficient in a single component of the complement system may develop associated changes in other proteins. Thus, an alternative explanation for our results could be that the decreases in CDA observed in mice deficient in C3aR (Fig. 1A) or in C6 (Fig. 1C) may be secondary to decreased C5a levels in these mice, as possibly suggested by the data expressed in Fig. 5. This possibility will be explored in future studies.

In summary, we have for the first time directly compared, in a single strain of mice that are comparably backcrossed, the effects of three of the major effector pathways of complement activation that have been proposed to cause tissue injury. Notably, we determined each effector to be important as deficiencies in each led to decreased clinical disease activity and

protection from injury using histologic criteria. There may be important differences in the engagement of non-complement dependent downstream pathways of inflammation that occur in some strains of mice in the absence of C3aR, C5aR, or C6 protein. However, a shared final effect in these strains may be enhanced local IgG binding with secondary C3 deposition, the latter possibly occurring through amplification mediated by the AP.

Supplementary Material

Refer to Web version on PubMed Central for supplementary material.

Acknowledgments

The authors thank: Ms. Jessica Nicholas for assisting in various complement ELISA assays, determining clinical disease scores and breeding various gene knockout mice; Ms. Nicole Spoelstra, Laser Capture Microscopy Core, Cancer Center, University of Colorado Denver-AMC for technical advice; Ms. Umarani Pugazhenthi, PCR Core University of Colorado Denver-AMC for performing quantitative RT-PCR on samples used in this study and Mr. Gaurav Mehta for taking histology pictures and adding a magnification scale bar.

This work was supported by NIH grant AR051749 to V.M. Holers.

Abbreviations used in this paper

CP	classical pathway
AP	alternative pathway
LP	lectin pathway
MAC or C5b-9	membrane attack complex
C6-def mice	C6 deficient mice
CAIA	collagen antibody-induced arthritis
CIA	collagen-induced arthritis
CII	type II collagen
DAS	disease activity score
AJM	all joint mean
IC	immune complex
NBF	neutral buffered formalin
RA	rheumatoid arthritis

References

1. Feldmann M, Brennan FM, Maini RN. Rheumatoid arthritis. Cell. 1996; 85:307–310. [PubMed: 8616886]
2. Firestein GS. Evolving concepts of rheumatoid arthritis. Nature. 2003; 423:356–361. [PubMed: 12748655]
3. Banda NK, Takahashi K, Wood AK, Holers VM, Arend WP. Pathogenic complement activation in collagen antibody-induced arthritis in mice requires amplification by the alternative pathway. J Immunol. 2007; 179:4101–4109. [PubMed: 17785849]
4. Banda NK, Takahashi M, Levitt B, Glogowska M, Nicholas J, Takahashi K, Stahl GL, Fujita T, Arend WP, Holers VM. Essential role of complement mannose-binding lectin-associated serine proteases-1/3 in the murine collagen antibody-induced model of inflammatory arthritis. J Immunol. 2010; 185:5598–5606. [PubMed: 20870940]

5. Banda NK, Thurman JM, Kraus D, Wood A, Carroll MC, Arend WP, Holers VM. Alternative complement pathway activation is essential for inflammation and joint destruction in the passive transfer model of collagen-induced arthritis. J Immunol. 2006; 177:1904–1912. [PubMed: 16849503]
6. Hietala MA, Jonsson IM, Tarkowski A, Kleinau S, Pekna M. Complement deficiency ameliorates collagen-induced arthritis in mice. J Immunol. 2002; 169:454–459. [PubMed: 12077276]
7. Ji H, Ohmura K, Mahmood U, Lee DM, Hofhuis FM, Boackle SA, Takahashi K, Holers VM, Walport M, Gerard C, Ezekowitz A, Carroll MC, Brenner M, Weissleder R, Verbeek JS, Duchatelle V, Degott C, Benoist C, Mathis D. Arthritis critically dependent on innate immune system players. Immunity. 2002; 16:157–168. [PubMed: 11869678]
8. Nandakumar KS, Holmdahl R. Antibody-induced arthritis: disease mechanisms and genes involved at the effector phase of arthritis. Arthritis Res Ther. 2006; 8:223. [PubMed: 17254316]
9. Hietala MA, Nandakumar KS, Persson L, Fahlen S, Holmdahl R, Pekna M. Complement activation by both classical and alternative pathways is critical for the effector phase of arthritis. Eur J Immunol. 2004; 34:1208–1216. [PubMed: 15048732]
10. Guo RF, Ward PA. Role of C5a in inflammatory responses. Annu Rev Immunol. 2005; 23:821–852. [PubMed: 15771587]
11. Haas PJ, van Strijp J. Anaphylatoxins: their role in bacterial infection and inflammation. Immunol Res. 2007; 37:161–175. [PubMed: 17873401]
12. Humbles AA, Lu B, Nilsson CA, Lilly C, Israel E, Fujiwara Y, Gerard NP, Gerard C. A role for the C3a anaphylatoxin receptor in the effector phase of asthma. Nature. 2000; 406:998–1001. [PubMed: 10984054]
13. Kohl J, Wills-Karp M. A dual role for complement in allergic asthma. Curr Opin Pharmacol. 2007; 7:283–289. [PubMed: 17475559]
14. Markiewski MM, DeAngelis RA, Benencia F, Ricklin-Lichtsteiner SK, Koutoulaki A, Gerard C, Coukos G, Lambris JD. Modulation of the antitumor immune response by complement. Nat Immunol. 2008; 9:1225–1235. [PubMed: 18820683]
15. Hsu MH, Ember JA, Wang M, Prossnitz ER, Hugli TE, Ye RD. Cloning and functional characterization of the mouse C3a anaphylatoxin receptor gene. Immunogenetics. 1997; 47:64–72. [PubMed: 9382922]
16. Perret JJ, Raspe E, Vassart G, Parmentier M. Cloning and functional expression of the canine anaphylatoxin C5a receptor. Evidence for high interspecies variability. Biochem J. 1992; 288(Pt 3):911–917. [PubMed: 1472004]
17. Cain SA, Monk PN. The orphan receptor C5L2 has high affinity binding sites for complement fragments C5a and C5a des-Arg(74). J Biol Chem. 2002; 277:7165–7169. [PubMed: 11773063]
18. Gerard NP, Lu B, Liu P, Craig S, Fujiwara Y, Okinaga S, Gerard C. An anti-inflammatory function for the complement anaphylatoxin C5a-binding protein, C5L2. J Biol Chem. 2005; 280:39677–39680. [PubMed: 16204243]
19. Ohno M, Hirata T, Enomoto M, Araki T, Ishimaru H, Takahashi TA. A putative chemoattractant receptor, C5L2, is expressed in granulocyte and immature dendritic cells, but not in mature dendritic cells. Mol Immunol. 2000; 37:407–412. [PubMed: 11090875]
20. Chen NJ, Mirtsos C, Suh D, Lu YC, Lin WJ, McKerlie C, Lee T, Baribault H, Tian H, Yeh WC. C5L2 is critical for the biological activities of the anaphylatoxins C5a and C3a. Nature. 2007; 446:203–207. [PubMed: 17322907]
21. Okinaga S, Slattery D, Humbles A, Zsengeller Z, Morteau O, Kinrade MB, Brodbeck RM, Krause JE, Choe HR, Gerard NP, Gerard C. C5L2, a nonsignaling C5A binding protein. Biochemistry. 2003; 42:9406–9415. [PubMed: 12899627]
22. Mastellos D, Lambris JD. Complement: more than a 'guard' against invading pathogens? Trends Immunol. 2002; 23:485–491. [PubMed: 12297420]
23. Liszewski MK, Kemper C, Price JD, Atkinson JP. Emerging roles and new functions of CD46. Springer Semin Immunopathol. 2005; 27:345–358. [PubMed: 16200405]
24. Kirchhoff K, Weinmann O, Zwirner J, Begemann G, Gotze O, Kapp A, Werfel T. Detection of anaphylatoxin receptors on CD83+ dendritic cells derived from human skin. Immunology. 2001; 103:210–217. [PubMed: 11412308]

25. Thangam EB, Venkatesha RT, Zaidi AK, Jordan-Sciutto KL, Goncharov DA, Krymskaya VP, Amrani Y, Panettieri RA Jr, Ali H. Airway smooth muscle cells enhance C3a-induced mast cell degranulation following cell-cell contact. FASEB J. 2005; 19:798–800. [PubMed: 15758041]
26. Chenoweth DE, Hugli TE. Demonstration of specific C5a receptor on intact human polymorphonuclear leukocytes. Proc Natl Acad Sci U S A. 1978; 75:3943–3947. [PubMed: 279010]
27. Soruri A, Grigat J, Kiafard Z, Zwirner J. Mast cell activation is characterized by upregulation of a functional anaphylatoxin C5a receptor. BMC Immunol. 2008; 9:29. [PubMed: 18559098]
28. Mikrou A, Zarkadis IK. Cloning of the sixth complement component and, spatial and temporal expression profile of MAC structural and regulatory genes in chicken. Dev Comp Immunol. 2010; 34:485–490. [PubMed: 20067805]
29. Morgan BP. Complement membrane attack on nucleated cells: resistance, recovery and non-lethal effects. Biochem J. 1999; 264:1–14. [PubMed: 2690818]
30. Nauta AJ, Daha MR, Tijsma O, van de Water B, Tedesco F, Roos A. The membrane attack complex of complement induces caspase activation and apoptosis. Eur J Immunol. 2002; 32:783–792. [PubMed: 11870622]
31. Rus HG, Niculescu FI, Shin ML. Role of the C5b-9 complement complex in cell cycle and apoptosis. Immunol Rev. 2001; 180:49–55. [PubMed: 11414362]
32. Tramontini NL, Kuipers PJ, Huber CM, Murphy K, Naylor KB, Broady AJ, Kilgore KS. Modulation of leukocyte recruitment and IL-8 expression by the membrane attack complex of complement (C5b-9) in a rabbit model of antigen-induced arthritis. Inflammation. 2002; 26:311–319. [PubMed: 12546141]
33. Matsumoto I, Staub A, Benoist C, Mathis D. Arthritis provoked by linked T and B cell recognition of a glycolytic enzyme. Science. 1999; 286:1732–1735. [PubMed: 10576739]
34. Tramontini N, Huber C, Liu-Bryan R, Terkeltaub RA, Kilgore KS. Central role of complement membrane attack complex in monosodium urate crystal-induced neutrophilic rabbit knee synovitis. Arthritis Rheum. 2004; 50:2633–2639. [PubMed: 15334478]
35. Bora PS, Sohn JH, Cruz JM, Jha P, Nishihori H, Wang Y, Kaliappan S, Kaplan HJ, Bora NS. Role of complement and complement membrane attack complex in laser-induced choroidal neovascularization. J Immunol. 2005; 174:491–497. [PubMed: 15611275]
36. Biesecker G, Gomez CM. Inhibition of acute passive transfer experimental autoimmune myasthenia gravis with Fab antibody to complement C6. J Immunol. 1989; 142:2654–2659. [PubMed: 2703710]
37. Orren A, Wallace ME, Hobart MJ, Lachmann PJ. C6 polymorphism and C6 deficiency in site strains of the mutant-prone Peru-Copprock mice. Complement Inflamm. 1989; 6:295–296.
38. Bhole D, Stahl GL. Molecular basis for complement component 6 (C6) deficiency in rats and mice. Immunobiology. 2004; 209:559–568. [PubMed: 15568620]
39. Banda NK, Levitt B, Glogowska MJ, Thurman JM, Takahashi K, Stahl GL, Tomlinson S, Arend WP, Holers VM. Targeted inhibition of the complement alternative pathway with complement receptor 2 and factor H attenuates collagen antibody-induced arthritis in mice. J Immunol. 2009; 183:5928–5937. [PubMed: 19828624]
40. Grant EP, Picarella D, Burwell T, Delaney T, Croci A, Avitahl N, Humbles AA, Gutierrez-Ramos JC, Briskin M, Gerard C, Coyle AJ. Essential role for the C5a receptor in regulating the effector phase of synovial infiltration and joint destruction in experimental arthritis. J Exp Med. 2002; 196:1461–1471. [PubMed: 12461081]
41. Soruri A, Kim S, Kiafard Z, Zwirner J. Characterization of C5aR expression on murine myeloid and lymphoid cells by the use of a novel monoclonal antibody. Immunol Lett. 2003; 88:47–52. [PubMed: 12853161]
42. Cavaillon JM, Fitting C, Haeffner-Cavaillon N. Recombinant C5a enhances interleukin 1 and tumor necrosis factor release by lipopolysaccharide-stimulated monocytes and macrophages. Eur J Immunol. 1990; 20:253–257. [PubMed: 1690130]
43. Skokowa J, Ali SR, Felda O, Kumar V, Konrad S, Shushakova N, Schmidt RE, Piekorz RP, Nurnberg B, Spicher K, Birnbaumer L, Zwirner J, Claassens JW, Verbeek JS, van Rooijen N, Kohl J, Gessner JE. Macrophages induce the inflammatory response in the pulmonary Arthus

reaction through G alpha i2 activation that controls C5aR and Fc receptor cooperation. J Immunol. 2005; 174:3041–3050. [PubMed: 15728518]

44. Takabayashi T, Vannier E, Clark BD, Margolis NH, Dinarello CA, Burke JF, Gelfand JA. A new biologic role for C3a and C3a desArg: regulation of TNF-alpha and IL-1 beta synthesis. J Immunol. 1996; 156:3455–3460. [PubMed: 8617973]
45. Ruan BH, Li X, Winkler AR, Cunningham KM, Kuai J, Greco RM, Nocka KH, Fitz LJ, Wright JF, Pittman DD, Tan XY, Paulsen JE, Lin LL, Winkler DG. Complement C3a, CpG oligos, and DNA/C3a complex stimulate IFN-alpha production in a receptor for advanced glycation end product-dependent manner. J Immunol. 2010; 185:4213–4222. [PubMed: 20817881]
46. Sunahori K, Yamamura M, Yamana J, Takasugi K, Kawashima M, Makino H. Increased expression of receptor for advanced glycation end products by synovial tissue macrophages in rheumatoid arthritis. Arthritis Rheum. 2006; 54:97–104. [PubMed: 16385501]
47. Watson WC, Brown PS, Pitcock JA, Townes AS. Passive transfer studies with type II collagen antibody in B10.D2/old and new line and C57Bl/6 normal and beige (Chediak-Higashi) strains: evidence of important roles for C5 and multiple inflammatory cell types in the development of erosive arthritis. Arthritis Rheum. 1987; 30:460–465. [PubMed: 3580014]
48. Camous L, Roumenina L, Bigot S, Brachemi S, Fremeaux-Bacchi V, Lesavre P, Halbwachs-Mecarelli L. Complement alternative pathway acts as a positive feedback amplification of neutrophil activation. Blood. 2011; 117:1340–1349. [PubMed: 21063021]
49. Girardi G, Berman J, Redecha P, Spruce L, Thurman JM, Kraus D, Hollmann TJ, Casali P, Caroll MC, Wetsel RA, Lambris JD, Holers VM, Salmon JE. Complement C5a receptors and neutrophils mediate fetal injury in the antiphospholipid syndrome. J Clin Invest. 2003; 112:1644–1654. [PubMed: 14660741]

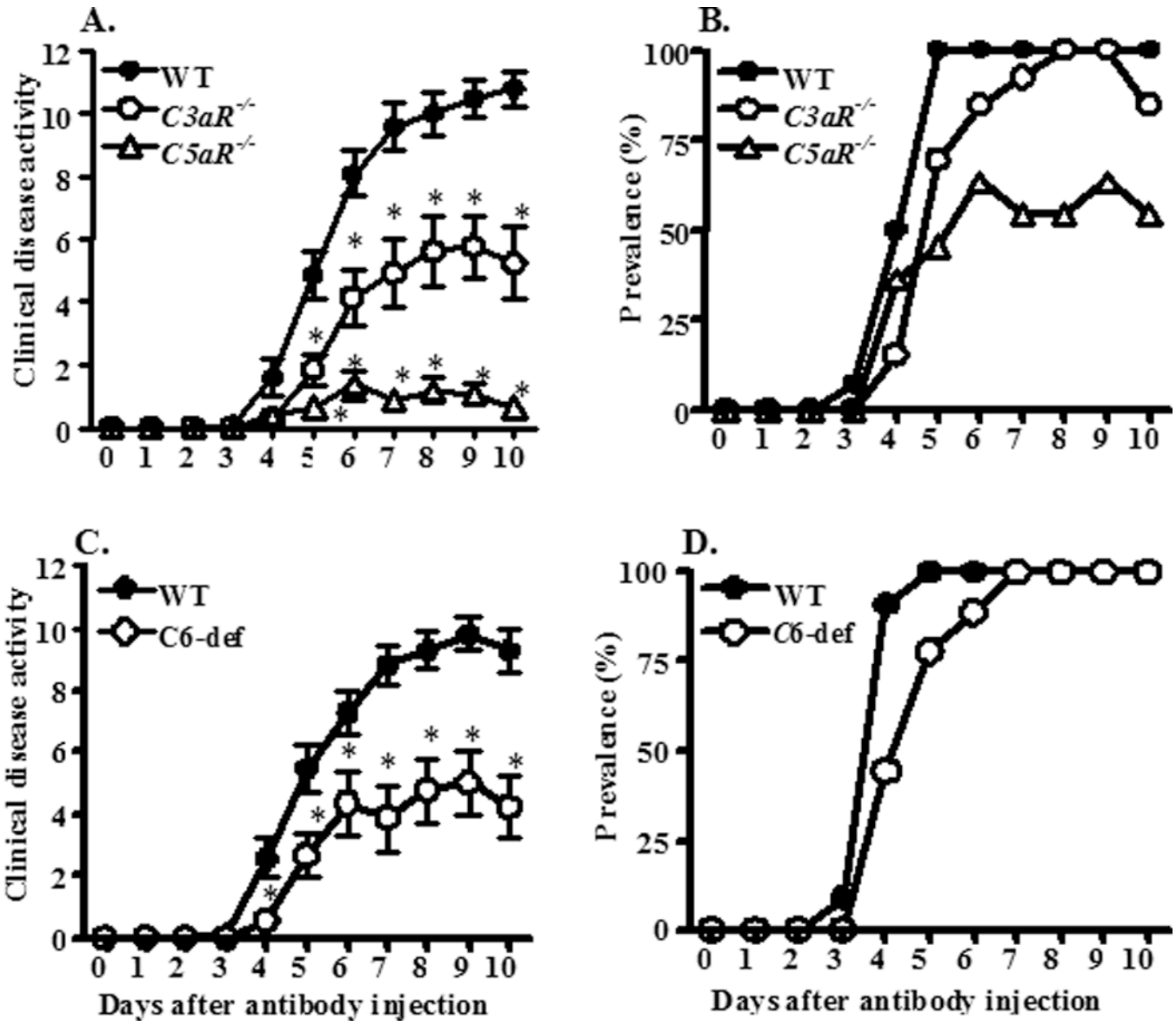

Figure 1.

CDA and prevalence of CAIA among WT, *C3aR*$^{-/-}$, *C5aR*$^{-/-}$, and C6-def mice. Arthrogen was injected i.p. on day 0 followed by an injection of LPS on day 3. Mice were evaluated daily by an observer blinded to the genotype of each mouse. Data are expressed as the CDA score (**A**, **C**) and prevalence of arthritis (**B**, **D**) vs. days after the injection. **A.** CDA among WT, *C3aR*$^{-/-}$, and *C5aR*$^{-/-}$ mice. **B.** The prevalence of disease in WT, *C3aR*$^{-/-}$, and *C5aR*$^{-/-}$ mice. **C.** CDA in WT and C6-def mice. **D.** The prevalence of disease in WT and C6-def mice. Data shown in **A** represent the mean ± SEM based on WT, n = 14; *C3aR*$^{-/-}$, n = 13; and *C5aR*$^{-/-}$, n = 11. Data shown in **B** represent the mean ± SEM based on WT, n = 11 and C6-def, n = 8. *$p < 0.05$ in *C3aR*$^{-/-}$, *C5aR*$^{-/-}$, and C6-def mice in comparison with CDA in WT from day 5 to day 10.

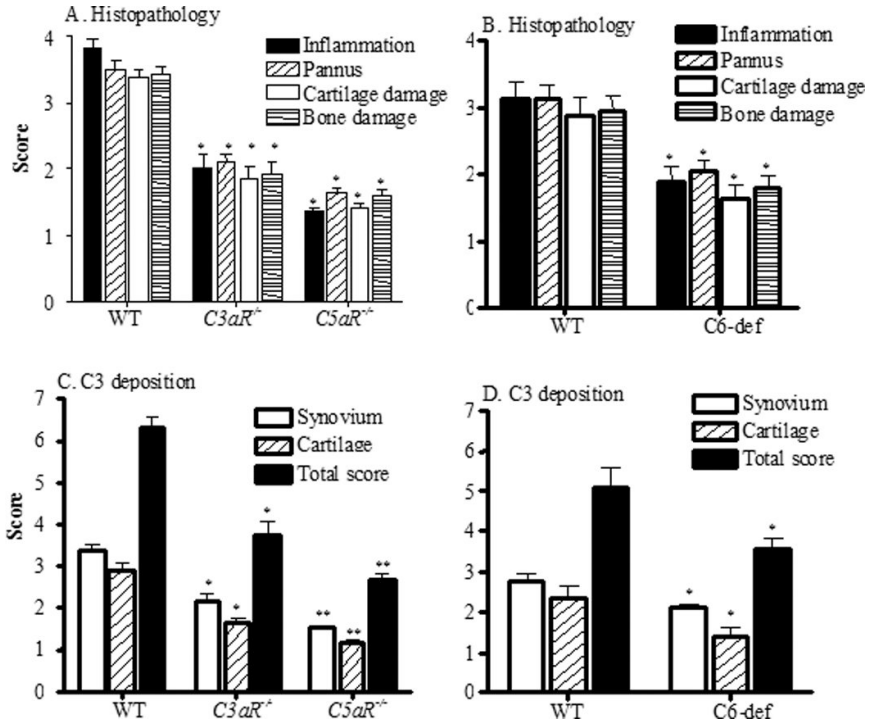

Figure 2.

Histopathological scores and C3 deposition in the joints of all WT, *C3aR*$^{-/-}$, *C5aR*$^{-/-}$, and C6-def mice. At day 10 following Arthrogen injection, mice were sacrificed. Histopathologic scoring for inflammation, pannus formation, cartilage and bone damage from five joints, including fore limbs (right and left) and one hind limb (right knee, ankle and paw), was performed following tissue processing and Toluidine-blue staining of sections. **A.** Individual components of histopathologic scores from WT (n =14), *C3aR*$^{-/-}$(n =13), and *C5aR*$^{-/-}$ (n =11) mice. **B.** Histopathologic scores from all five joints of WT (n = 11) and C6-def (n = 8) mice. Knee joints of mice with CAIA were used to examine for C3 deposition. **C.** C3 deposition in knee joints in the synovium, on the surface of cartilage, and total scores (synovium plus cartilage) from WT, *C3aR*$^{-/-}$, and *C5aR*$^{-/-}$ mice. **D.** C3 deposition in the synovium and on the surface of cartilage from WT and C6-def mice. All data are represented as scores (mean ± SEM). *$p < 0.05$ in comparison to WT mice of individual histopathologic and C3 deposition scores. **$p < 0.05$ inter-group comparison of individual histopathologic and C3 deposition scores between *C5aR*$^{-/-}$ and *C3aR*$^{-/-}$ or C6-def mice

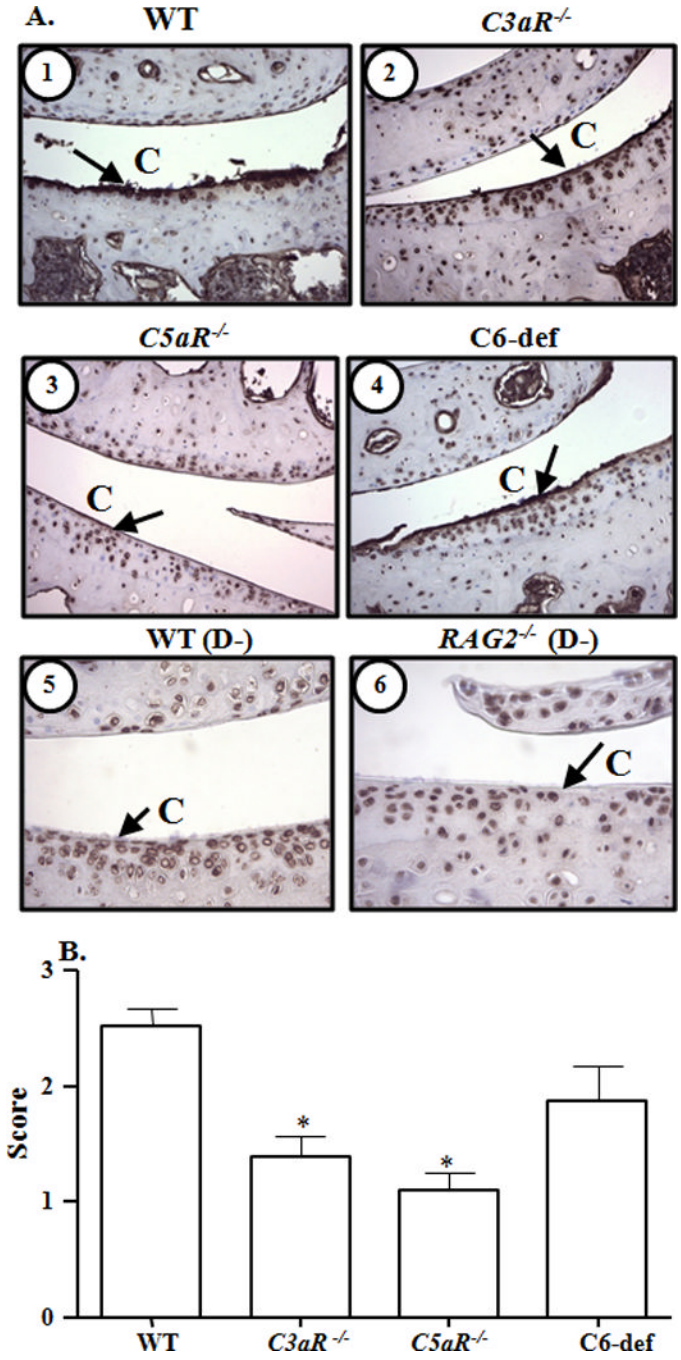

Figure 3.

Immunohistochemical analysis of IgG deposition on the surface of cartilage from knee joints of WT, *C3aR*$^{-/-}$, *C5aR*$^{-/-}$, and C6-def mice with CAIA. **A.** Cartilage surface in the knee joints is marked as (C). IgG deposition (brown color stain) on the cartilage surface is shown by black arrows. Top panel left to right, cartilage surface from the knee joints of: **1.** WT mice, and **2.** *C3aR*$^{-/-}$ mice, both with CAIA. Central panel left to right: **3.** *C5aR*$^{-/-}$ mice, and **4.** C6-def mice, both with CAIA. Bottom panel left to right: **5.** C57BL/6 mice, and **6.** *RAG2*$^{-/-}$ mice, both without CAIA. Magnification in all pictures was 40X to show the surface of cartilage. **B**. Quantification of IgG deposition in the joints of all WT, *C3aR*$^{-/-}$, *C5aR*$^{-/-}$, and C6-def mice. At day 10 following Arthrogen injection, mice were sacrificed

and IgG deposition was scored on a scale of 0–3. Endogenous IgG was considered as normal background levels and knee joints from *RAG2*$^{-/-}$ mice on a C57BL/6 background naturally lacking IgG were used as negative controls. All data represent the mean ± SEM based on n = 21 for WT, n = 13 for *C3aR*$^{-/-}$, n = 11 for *C5aR*$^{-/-}$, and n= 8 for C6-def mice. *$p < 0.001$ in comparison with WT mice, by Tukey's multiple comparison test.

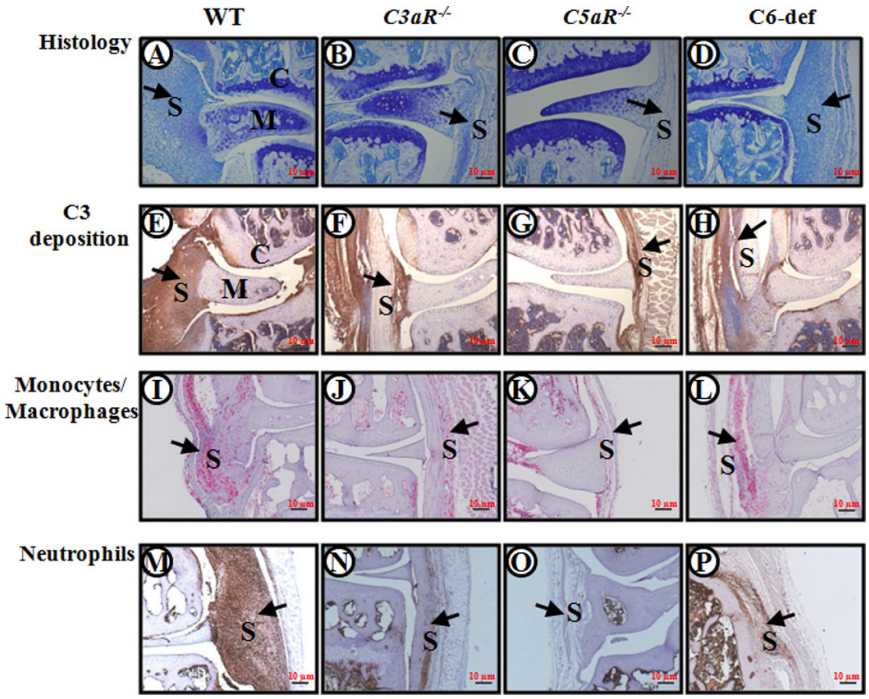

Figure 4.

Histopathology, C3 deposition, monocyte/macrophage infiltration, and neutrophil infiltration from WT, *C3aR*$^{-/-}$, *C5aR*$^{-/-}$, and C6-def mice with CAIA. Knee joints with maximum CDA scores from WT, *C3aR*$^{-/-}$, *C5aR*$^{-/-}$, and C6-def mice with CAIA were selected. Areas of synovium (S), cartilage (C), and meniscus (M) are identified. The black arrows all point to the synovium. From left to right, knee joints of WT, *C3aR*$^{-/-}$, *C5aR*$^{-/-}$, and C6-def mice stained with Toluidine-blue (blue color) are shown in A, B, C and D. Similarly, knee joints with C3 deposition (brown color) are shown in E, F, G and H; knee joints stained with F4/80 (red color) for monocytes/macrophages are shown in I, J, K and L; and knee joints stained with neutrophil (brown color) surface marker are shown in M, N, O and P. Magnification for all pictures was 10X (a magnification red scale bar at 10X of 10 μm (0.01mm) is included on the lower right hand corner in all frames).

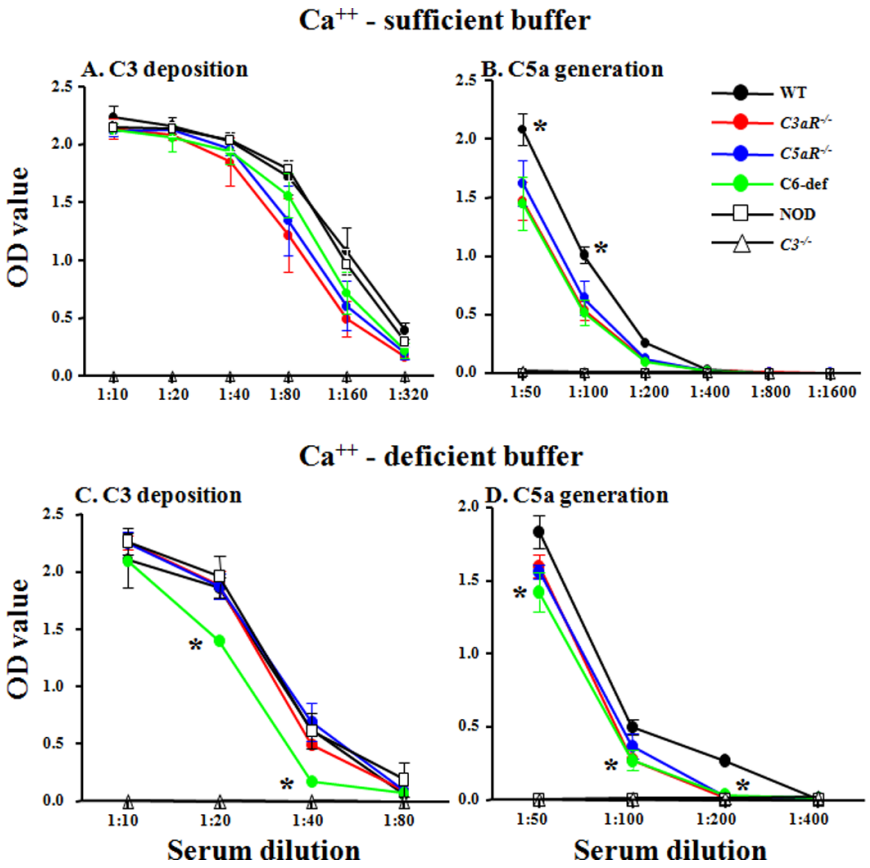

Figure 5.

Anti-collagen Ab-induced activation of the AP in vitro using sera from WT, *C3aR*$^{-/-}$, *C5aR*$^{-/-}$, and C6-def mice without CAIA. C3 deposition and C5a generation were measured by incubating sera from WT, *C3aR*$^{-/-}$, *C5aR*$^{-/-}$, and C6-def mice on ELISA plates pre-coated with four anti-collagen mAb specific for bovine type II collagen. The experiments were performed with the same sera serially diluted 2-fold in Ca^{++}-sufficient buffer (panels A and B), where all three complement activation pathways were active, or with Ca^{++}-deficient buffer (panels C and D), where only the AP was active. Sera from *C3*$^{-/-}$ and non-obese diabetic (NOD) mice were used as negative controls for C3 deposition and C5a generation, respectively. The X-axis shows various serum dilutions and the Y-axis shows mean OD values. **A.** C3 deposition on the ELISA plates using Ca^{++}-sufficient buffer. **B.** C5a generation in the supernatant using Ca^{++}-sufficient buffer. **C.** C3 deposition using Ca^{++}-deficient buffer. **D.** C5a generation using Ca^{++}-deficient buffer. All data are expressed in optical density units (OD). The baseline levels of C5a in the sera before incubation on the mAb to CII were subtracted from the total C5a measured at the end of each experiment. The data shown here represent the mean ± SEM based experiments with Ca^{++}-sufficient buffer: n = 4 for WT, n = 4 for *C3aR*$^{-/-}$, n = 4 for *C5aR*$^{-/-}$, n = 3 for *C6*$^{-/-}$, n = 4 for NOD, and n = 4 for *C3*$^{-/-}$ mice. The data for experiments using Ca^{++}-deficient buffer represent the mean + SEM based on: n = 5 for WT, n = 5 for *C3aR*$^{-/-}$, n = 5 for *C5aR*$^{-/-}$, n = 5 for C6-def, n = 5 for NOD, and n = 5 for *C3*$^{-/-}$ mice. * = $p < 0.05$: in panel B for.each of the complement-deficient sera vs. WT; in panel C for sera from C6-def vs. WT mice; and in panel D for sera from C6-def vs. WT mice.

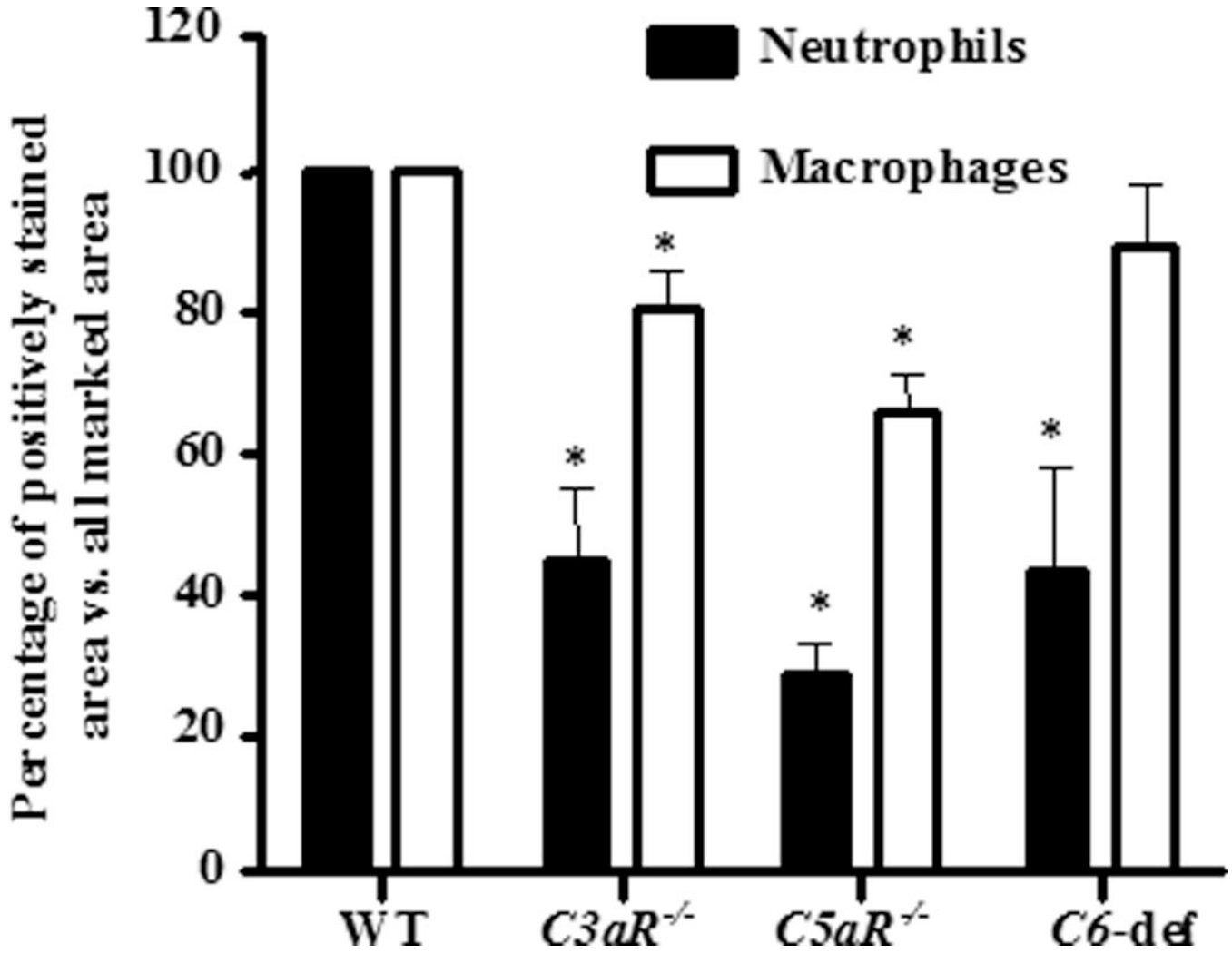

Figure 6.

Percentages of macrophages and neutrophils in the synovium of knee joints from WT, *C3aR*$^{-/-}$, *C5aR*$^{-/-}$, and C6-def mice with CAIA. All mice were sacrificed at day 10 and knee joints were stained using methods specific for macrophages and neutrophils. The percentages of macrophages and neutrophils in the synovium were calculated by image analysis quantitating the stained marked areas of neutrophils and macrophages in comparison to the total marked area of the synovium. All data shown here represent the mean ± SEM based on n = 14 for WT, n = 13 for *C3aR*$^{-/-}$, and n = 11 for *C5aR*$^{-/-}$. WT n = 11 and n= 8 for C6-def mice. *$p < 0.05$ in comparison with WT mice.

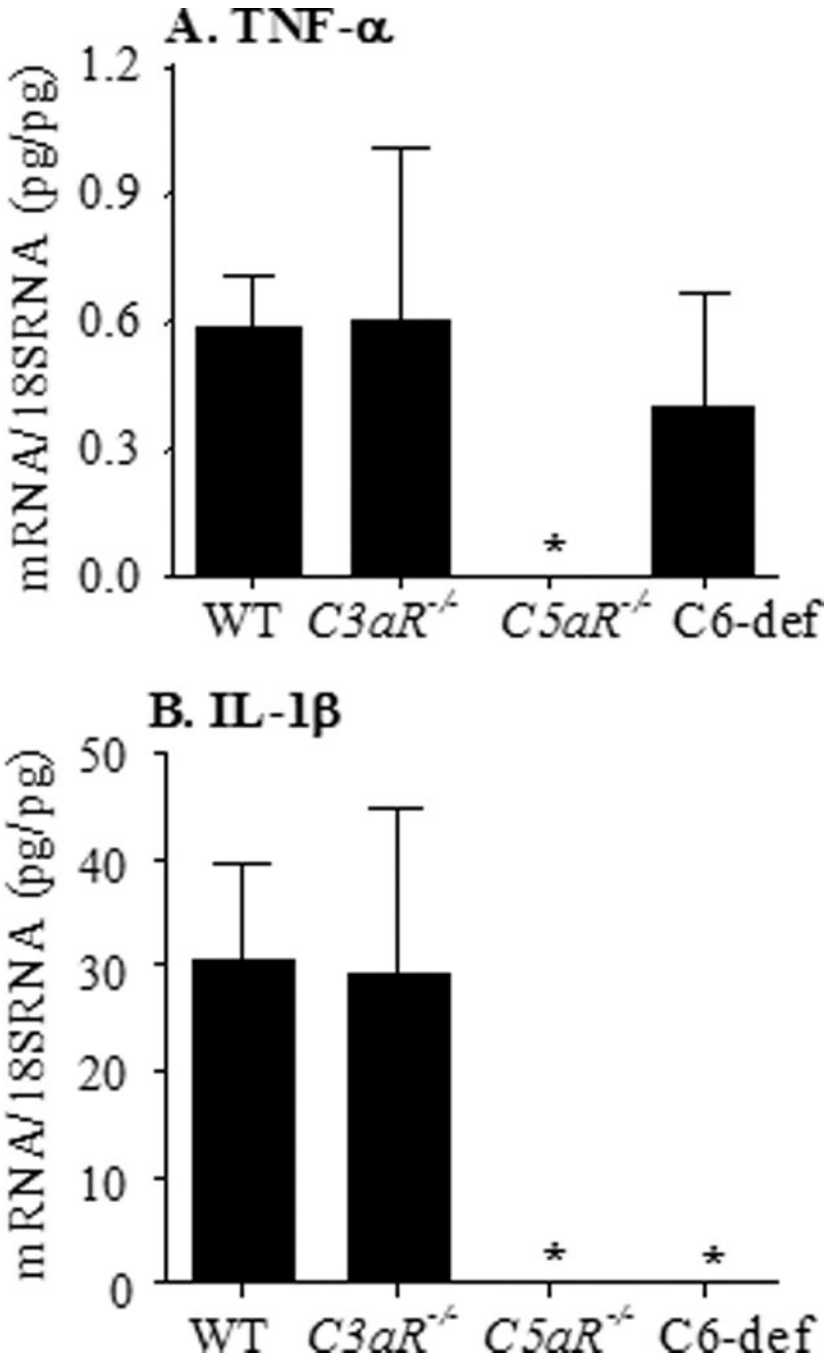

Figure 7.

mRNA levels of TNF-α and IL-1β in synovium obtained by LCM from the knee joints of WT, *C3aR*$^{-/-}$, *C5aR*$^{-/-}$, and C6-def mice with CAIA. The mRNA levels for synovial cytokines were measured by quantitative RT-PCR using cDNA made from aRNA, as described in Methods, with specific primers and probes for TNF-α (Fig. 7A) and IL-1β (Fig. 7B). The mRNA levels for each cytokine were expressed as specific mRNA (pg)/18s rRNA (pg). All data represent the mean ± SEM based on n = 5 for WT, n = 5 for *C3aR*$^{-/-}$, n = 3 for *C5aR*$^{-/-}$, and n = 6 for C6-def mice. *$p < 0.05$ in comparison with WT mice.

Table 1

Levels of complement components in sera from WT and complement component deficient mice[A]

Mice (n)	C1q	C3	C4	factor B	factor D
WT (23) [B]	0.502 ± 0.04	1.730 ± 0.09	1.086 ± 0.09	0.608 ± 0.03	1.721 ± 0.05
C3aR$^{-/-}$ (15) [B]	0.696 ± 0.04	1.674 ± 0.08	1.137 ± 0.08	0.539 ± 0.01	1.777 ± 0.05
p	*0.002*	*0.650*	*0.668*	*0.069*	*0.449*
C5aR$^{-/-}$ (14) [B]	0.567 ± 0.03	1.661 ± 0.08	0.742 ± 0.10	0.500 ± 0.04	1.751 ± 0.14
p	*0.227*	*0.571*	*0.014*	*0.0429*	*0.847*
C6-def (6)	0.536 ± 0.06	1.873 ± 0.22	1.009 ± 0.14	0.567 ± 0.01	1.618 ± 0.06
p	*0.654*	*0.563*	*0.786*	*0.249*	*0.197*

[A] Data are expressed as optical density units with mean ± SEM based on the indicated number of sera (n).

[B] WT mice used to measure factor B (n = 9); *C3aR*$^{-/-}$ (n=6); *C5aR*$^{-/-}$ (n = 6); [B] WT mice used to measure factor D (n=13).

All p-values for different complement components were compared with the corresponding values of WT mice. $p < 0.05$ were considered statistically significant.